

MRF Boundary Layer Parameterization

Melissa Goering
ATMO 595E
December 2, 2004

Outline

- Background for MRF PBL scheme
- WRF Input data
 - Constants (WRF and MRF PBL subroutine)
- MRF Output data
- Equations
 - Troen and Mahrt 1986
 - Hong and Pan 1996
 - Businger et al., 1971
 - Brost and Wyngaard 1978
- Sensitivity Analysis

Basic MRF PBL Parameterization

Vertical diffusion scheme MRF (prior 1996)

- There is no explicit boundary layer parameterization
- Diffusivity coefficients are parameterized as functions of the local Richardson number
- Thus the local-K approach (by Louis 1979) is used for BOTH boundary layer and free atmosphere
- Widely used because computationally cheap and produces reasonable results under typical atmospheric conditions
- However, the scheme cannot handle conditions when atmosphere is well mixed because of the countergradient fluxes. Thus, the method is not well behaved for unstable conditions.

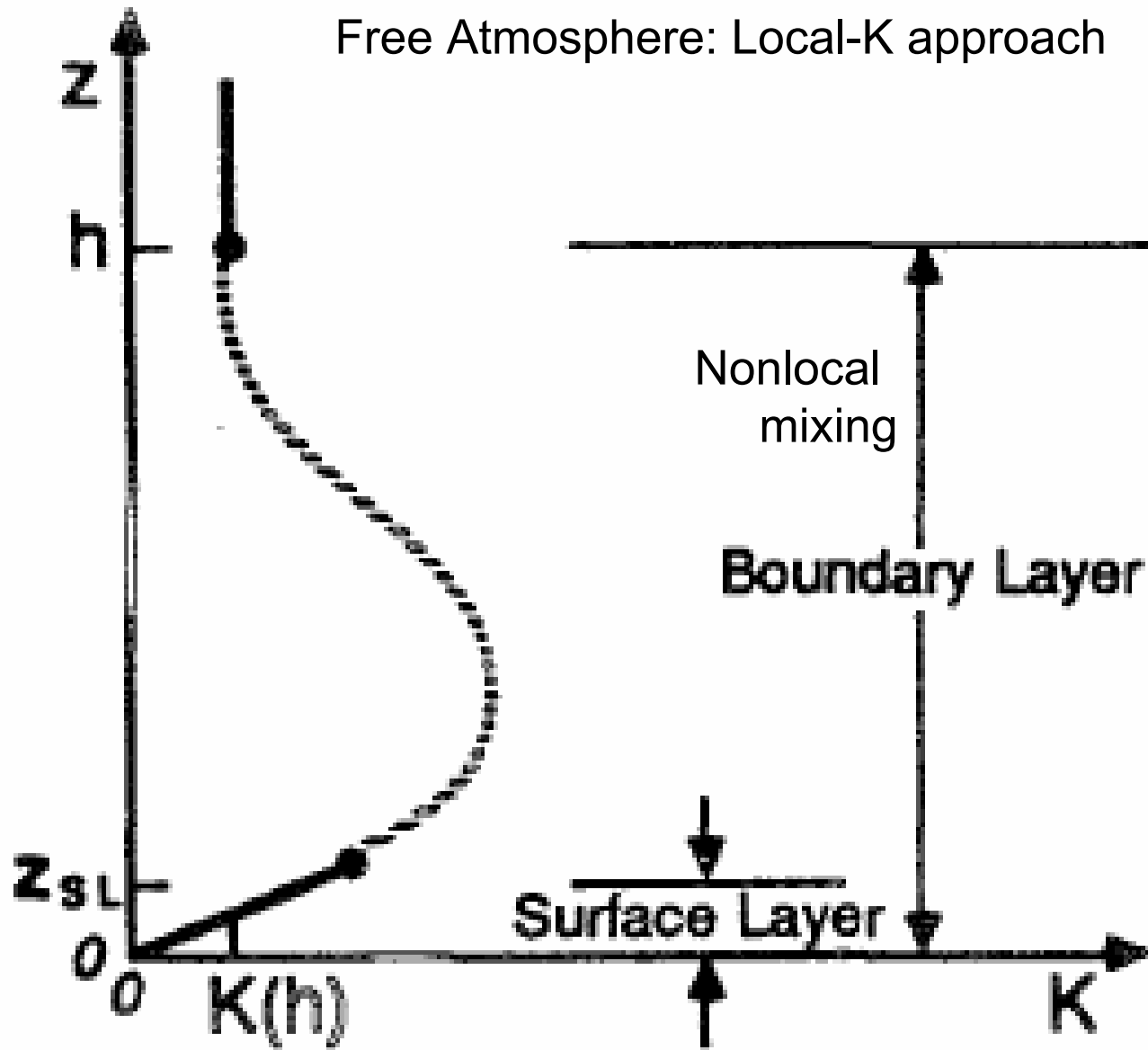
Basic MRF PBL Parameterization

Concept adapted by Troen and Mahrt, 1986*:

- Develop model where transport of mass and momentum in PBL is accomplished by large scale eddies and modeled by bulk properties of PBL instead of local prosperities
- Turbulent diffusivity coefficients are calculated from prescribed profile shape as function of boundary layer heights and scale parameters derived from similarity requirements
- Utilizes the results of the large-eddy simulation research and is computationally efficient

* Businger et al. 1971; Brost and Wyngaard 1978; Wyngaard and Brost 1984; Holtslag and Boville 1993;

Free Atmosphere: Local-K approach



WRF Input Data

U3D	3D u-velocity interpolated to theta points (m/s)
V3D	3D v-velocity interpolated to theta points (m/s)
TH3D	3D potential temperatures (K)
T3D	temperature (K)
QV3D	3D water vapor mixing ratio (kg/kg)
QC3D	3D cloud mixing ratio (kg/kg)
QI3D	3D ice mixing ratio (kg/kg)
P3D	3D pressure (Pa)
PI3D	3D exern function (dimensionless)
rr3D	3D dry air density (kg/m ³)
RUBLTEN	U tendency equation to PBL (m/s ²)
RVBLTEN	V tendency equation to PBL (m/s ²)
RTHBLTEN	Theta tendency equation to PBL (K/s)
RQVBLTEN	Qv tendency equation to PBL (kg/kg/s)
RQCBLTEN	Qc tendency equation to PBL (kg/kg/s)
RQIBLTEN	Qi tendency equation to PBL (kg/kg/s)
P_QI	species index for cloud ice
dz8w	dz between full levels
z	height above sea level (m)

WRF Input Data (continued)

PSFC	pressure at surface (Pa)
ZNT	roughness length (m) [land=0.10, water=0.001]
UST	u^* in similarity theory (m/s)
ZOL	z/L height over Monin-Obukhov length
HOL	PBL Height over Monin-Obukhov length
REGIME	flag indicating PBL regime (stable, unstable, etc)
PSIM	similarity stability function for momentum
PSIH	similarity stability function for heat
XLAND	land mask (1= land, 2 = water)
HFX	upward heat flux at the surface (W/m^2)
QFX	upward moisture flux at the surface ($\text{kg/m}^2/\text{s}$)
TSK	surface temperature (K)
GZ10Z0	$\log(z/z_0)$ where z_0 is roughness length
WSPD	wind speed at lowest model level (m/s)
BR	bulk Richardson number in surface layer
DT	time step seconds
DTMIN	time step minutes

WRF Input Constants

ROVCP	R/CP
R	gas constant for dry air (J/kg/K)
G	acceleration due to gravity (m/s ²)
ROVG	R/G
XLV	latent heat of vaporization (J/kg)
RV	gas constant for vaporization (J/kg)
rvovrd	R_v divided by R_d (dimensionless)
SVP1	constant saturation vapor pressure (KPa)
SVP2	constant saturation vapor pressure (dimensionless)
SVP3	constant saturation vapor pressure (K)
SVPT0	constant saturation vapor pressure (K)
EP1	constant for virtual temperature (Rv/Rd -1), 0.608
EP2	constant for specific humidity calculation, 0.628
KARMAN	Von Karman constant
EOMEG	angular velocity of earth's rotation (rad/s)
STBOLT	Stefan-Boltzman constant (W/m ² /K ⁴)

MRF PBL subroutine Constants

BRCR = 0.5

Critical Bulk Richardson number

RLAM = 150

**Asymptotic length scale 250m,
Hong and Pan1996 to 30m**

Rlmin = -100.0

Local gradient Ri to prevent unrealistic unstable

ZFmin = 1×10^{-8}

Minimum value allowed in equation $K_{zm}, (1 - z/h)$

PRmin = 0.5

Prandtl number bounded $0.5 < Pr < 4.0$

PRmax = 4.0

XKZmin = 0.01

Diffusivity coef. bounded between $0.01 < K_z < 1000 \text{ m}^2\text{s}^{-1}$

XKZmax = 1000.0

CFAC = 7.8

thermal excess b in equation based on observation

PFAC = 2.0

exponential p in equation based on observation

PRT = 1.0

Alpha5 = 5.0

constant in equation based on observation

Alpha16 = 16.0

constant in equation based on observation

CKZ = 0.001

XKA = 2.4×10^{-5}

SFCFRAC = 0.1

MRF PBL subroutine Output Data

U2DTEN	u tendency calculated
V2DTEN	v tendency calculated
T2DTEN	temperature tendency calculated
QV2DTEN	water vapor tendency calculated
QC2DTEN	cloud tendency calculated
QI2DTEN	ice tendency calculated
KPBL1D	boundary layer height (m)
PSIM	similarity stability function for momentum
PSIH	similarity stability function for heat
HFX	upward heat flux at the surface (W/m²)
QFX	upward moisture flux at the surface (kg/m²/s)
TSK	surface temperature (K)
ZNT	roughness length (m)
UST	u* in similarity theory (m/s)
ZOL	z/L height over Monin-Obukhov length
HOL	PBL Height over Monin-Obukhov length
REGIME	flag indicating PBL regime (stable, unstable, etc)

MRF Equations

- Nonlocal Diffusivity: Mixed layer
 - Stable Regime
 - Unstable Regime
- Calculation PBL
- Local-K approach: Free Atmosphere
 - Stable Regime
 - Unstable Regime
- Where did constants come from?
 - Kansas 1968
 - Minnesota 1973

Nonlocal Diffusivity

$$\theta_s = \theta_{\text{vs}} + \theta_T \left[= b \frac{\overline{(w' \theta'_v)_0}}{w_s h} \right],$$

stable

θ_T -virtual temperature excess near the surface, maximum limit of 3K

$$h = \text{Rib}_{\text{cr}} \frac{\theta_{\text{vs}} |U(h)|^2}{g(\theta_v(h) - \theta_s)},$$

h – is the boundary layer height and determined iteratively; $\text{Rib}_{\text{cr}} = 0.5$

$$w_s = u_{\text{ref}} \phi_m^{-1},$$

W_s – the mixed layer velocity scale, where UST calculated

$$\gamma_c = b \frac{\overline{(w' c')}}{w_s}$$

γ_c – countergradient calculated for θ and q , where $b=7.8$; term is small stable conditions

$$\frac{\partial C}{\partial t} = \frac{\partial}{\partial z} \left[K_c \left(\frac{\partial C}{\partial z} - \gamma_c \right) \right]$$

Calculate tendency

Nonlocal Diffusivity

$$L = \frac{-u_*^3}{k(g/\theta_{co})(\overline{w'\theta'_v})_0}$$

Monin-Obukov length

stable regime [$(\overline{w'\theta'_v})_0 > 0$],

$$\phi_m = \phi_r = \left(1 + 5 \frac{0.1h}{L}\right),$$

Turbulent velocity scale

$$w_s = u_* \phi_m^{-1},$$

$$K_{zm} = kw_s z \left(1 - \frac{z}{h}\right)^p$$

$$u_* = [(\overline{u'w'})_0^2 + (\overline{v'w'})_0^2]^{1/4}$$

Friction velocity

unstable and neutral conditions [$(\overline{w'\theta'_v})_0 \leq 0$],

$$\phi_m = \left(1 - 16 \frac{0.1h}{L}\right)^{-1/4}, \quad \text{for } u \text{ and } v$$
$$\phi_r = \left(1 - 16 \frac{0.1h}{L}\right)^{-1/2}, \quad \text{for } \theta \text{ and } q,$$

Prandtl number

$$\text{Pr} = \left(\frac{\phi_r}{\phi_m} + bk \frac{0.1h}{h}\right),$$

$$K_{zh} = K_{zm} / \text{Pr}$$

Local-K diffusivity

Calculate the vertical
wind shear and
mixing length

$$\left| \frac{\partial U}{\partial z} \right|$$

$$\frac{1}{l} = \frac{1}{kz} + \frac{1}{\lambda_0}$$

$$Rig = (g/\bar{\theta}_v) \partial \bar{\theta}_v / \partial z / [(\partial \bar{u} / \partial z)^2 + (\partial \bar{v} / \partial z)^2]$$

Rig < 0, Unstable

Rig > 0, Stable

h

$$f_r(Rig) = (1 + 16.0 Rig)^{-1/2}$$

$$f_r(Rig) = (1 + 5.0 Rig)^{-2}$$

$$Pr = 1.0 + 2.1 Rig$$

m

$$f_r(Rig) = (1 + 16.0 Rig)^{-1/4}$$

$$f_r(Rig) = (1 + 5.0 Rig)^{-2*Pr}$$

$$K_{m,l} = l^2 f_{m,l}(Rig) \left| \frac{\partial U}{\partial z} \right|$$

Where did they get those constants?

Kansas 1968 (Businger et al., 1971)

- site located in wheat farming country of southwestern Kansas
- 32m tower located in center of one mile square field of wheat stubble ~18cm tall
- Analyses suggest surface roughness length of ~2.4cm, zero plane displacement of ~10cm
- 34 runs analyzed with basic average period 15min

Businger et al., 1971

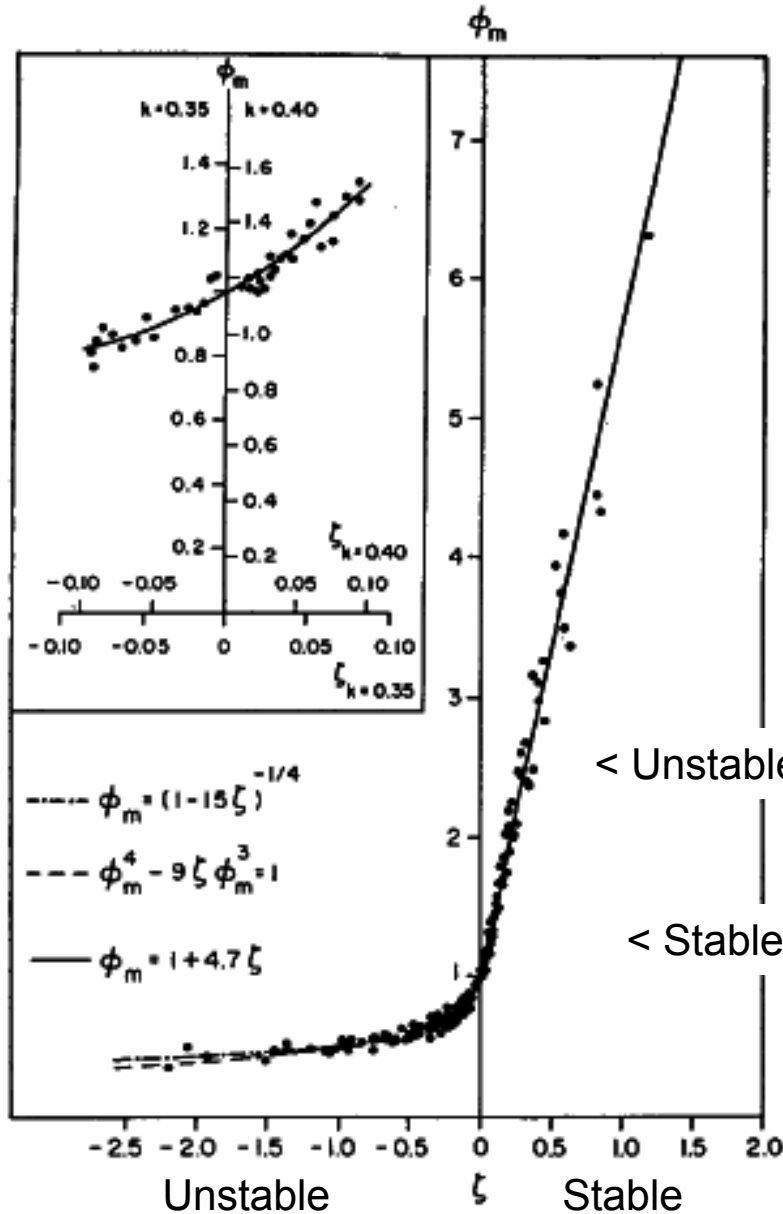


FIG. 1. Comparison of dimensionless wind shear observations with interpolation formulas.

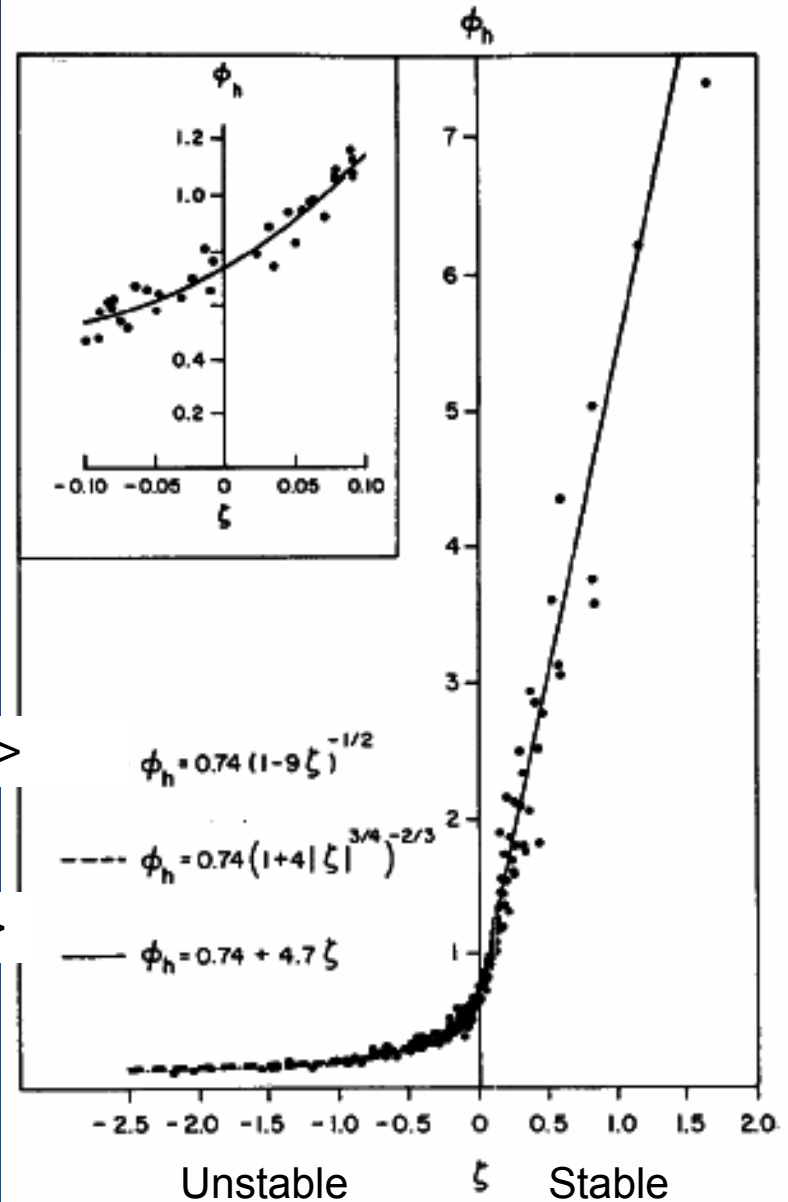


FIG. 2. Comparison of dimensionless temperature gradient observations with interpolation formulas.

Businger et al., 1971

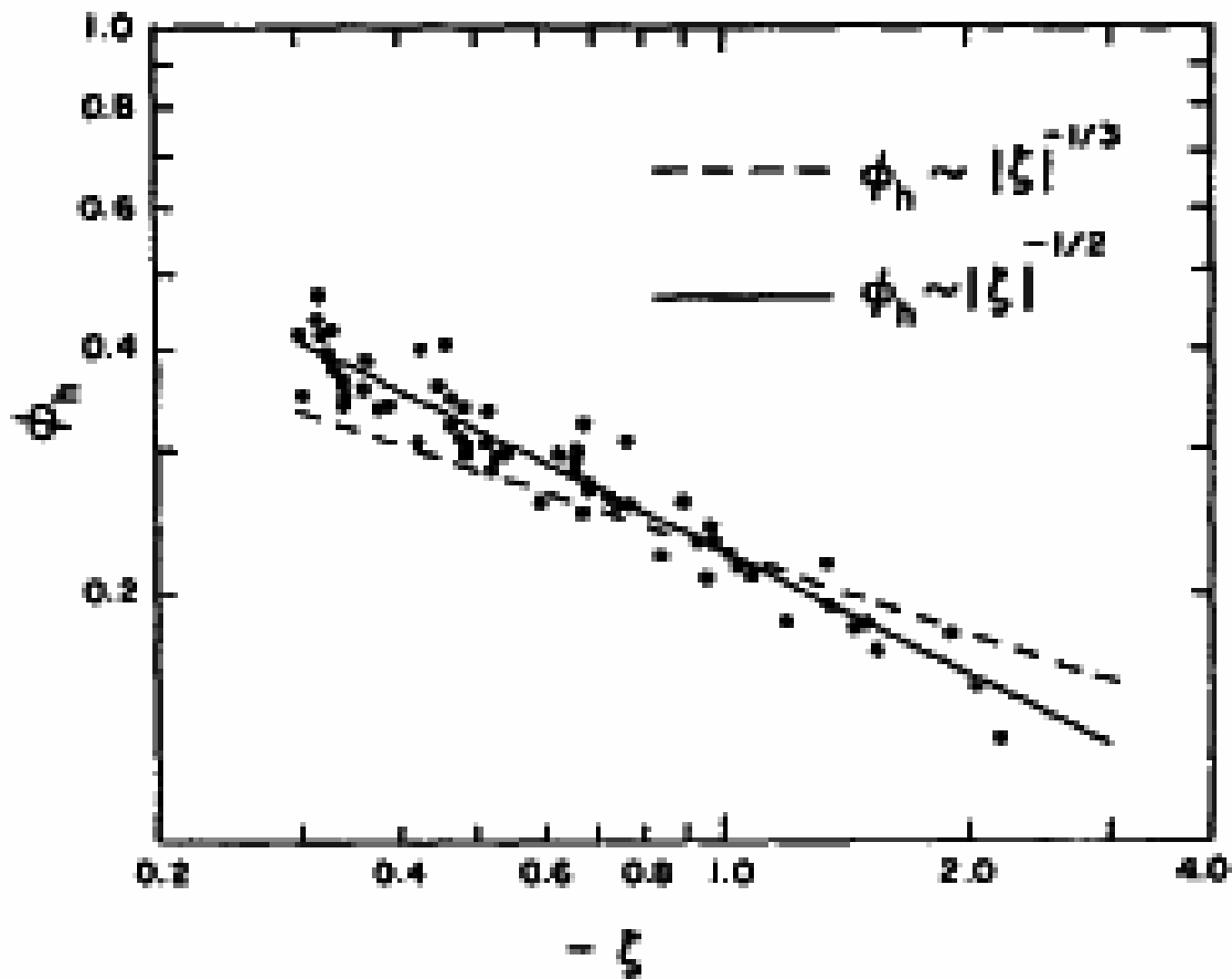


FIG. 3. The dimensionless temperature gradient under very unstable conditions.

Sensitivity Analysis

Evaluate role of countergradient term by removing thermal excess ($b=0.0$):

- Removing thermal excess ($b=0.0$), the nonlocal turbulent mixing due to the γ_c plays a role in stabilizing the structure and creates a deeper boundary layer depth (more clearly in mixing ratio)
- However, the γ_c is not fully responsible for difference between local and nonlocal and the cubic shape is also important in the nonlocal scheme
- Found that the impact of nonlocal mixing due to mixing ratio γ_c effect was negligible (no figure)

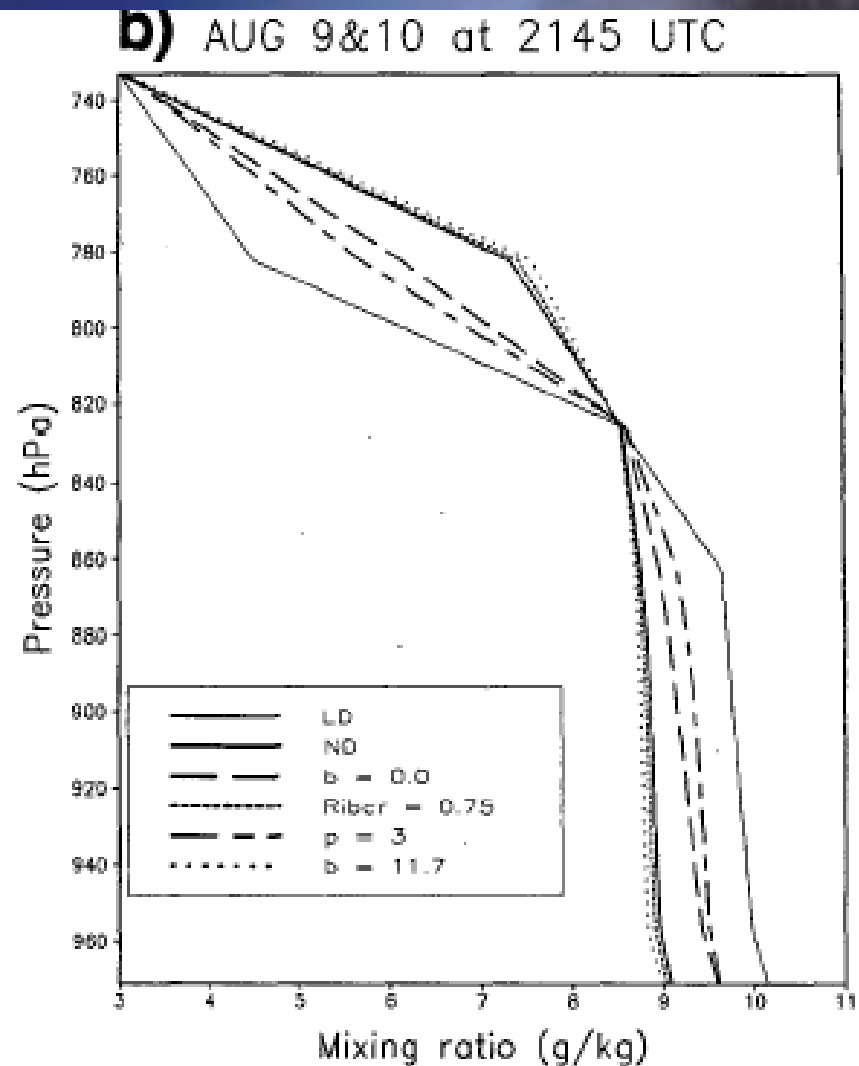
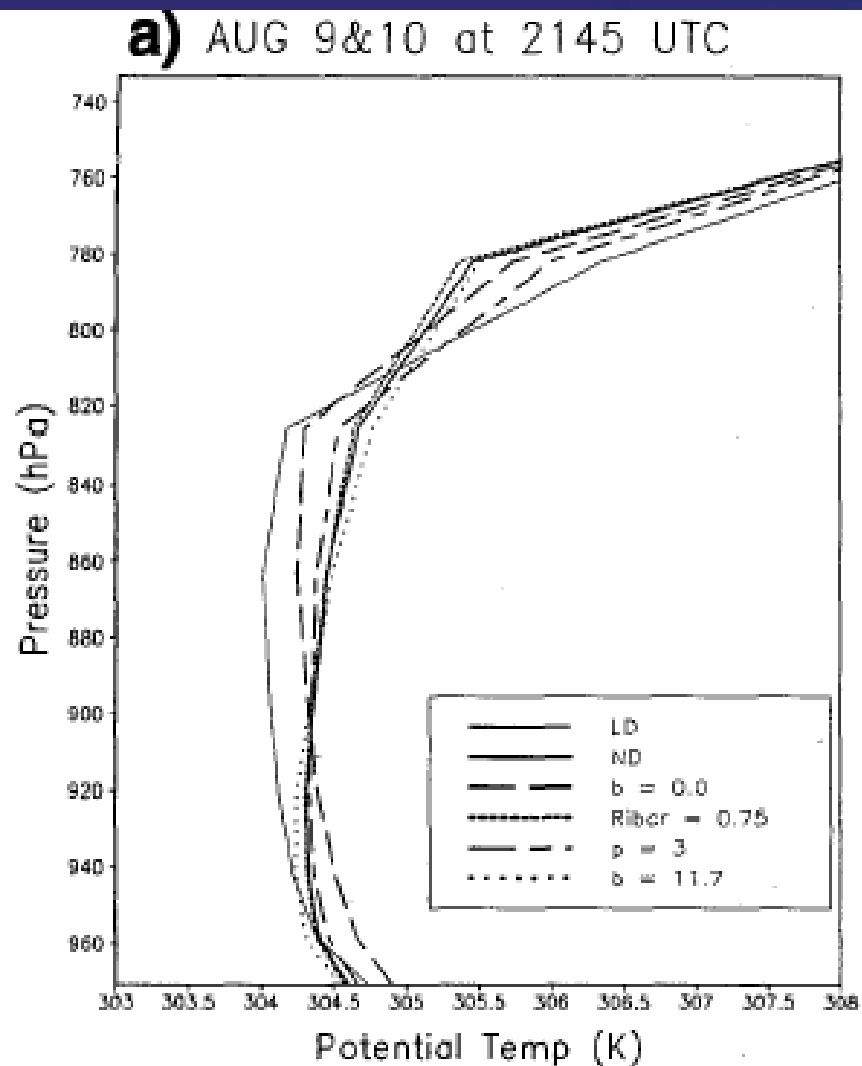


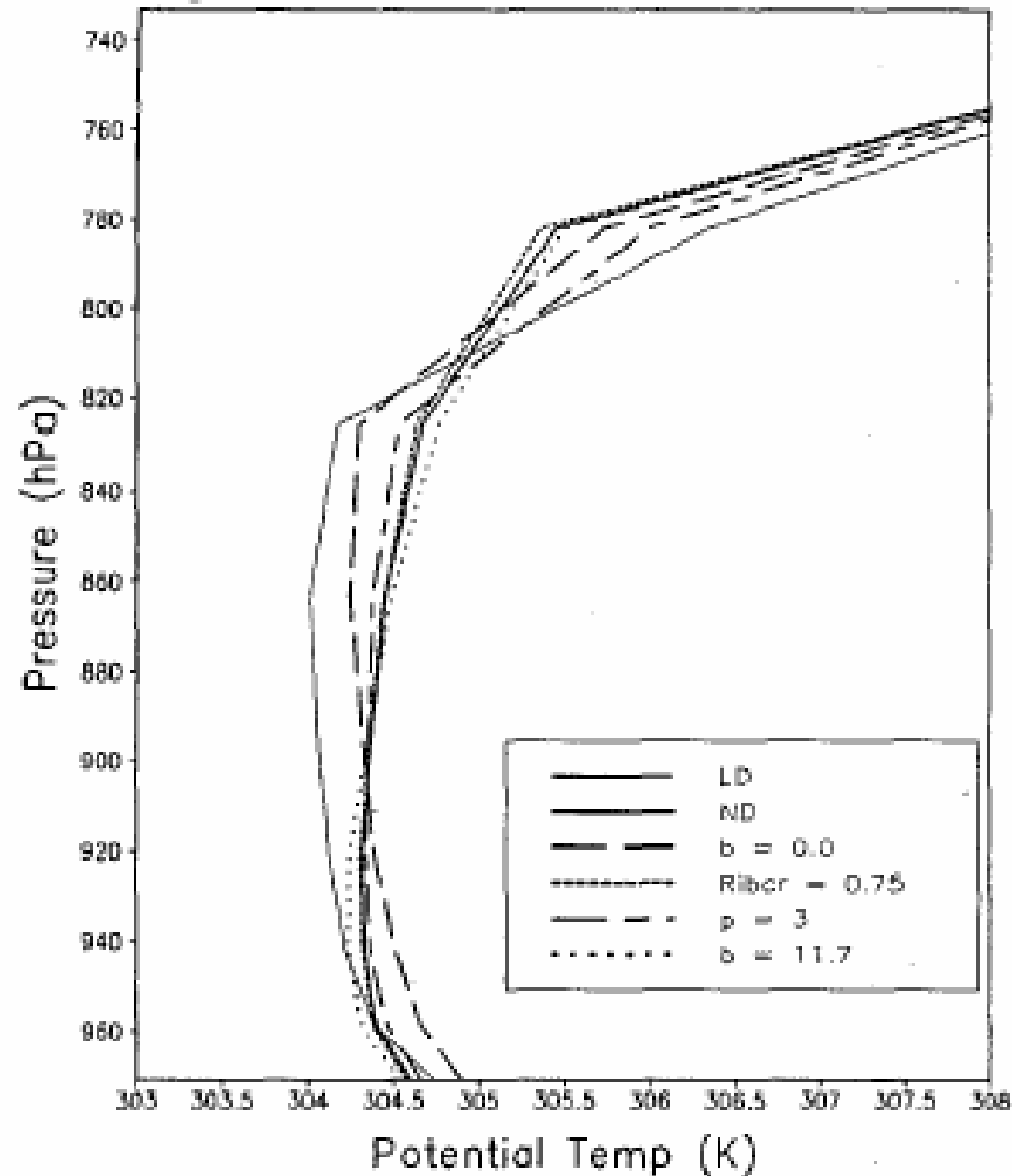
FIG. 5. Comparisons of boundary layer profiles of (a) potential temperature (K) and (b) mixing ratio (g kg^{-1}) for 9–10 August at 2145 UTC resulting from the local scheme experiment (light solid), the control nonlocal experiment (heavy solid), the experiment without the countergradient term ($b = 0$) (long dashed), with the increased Rib_{cr} (short dashed), with the increased p (dash-dotted), and with the increased b factor (dotted).

Sensitivity Analysis

Evaluate role of countergradient term by increasing thermal excess $b=[7.8,11.7]$:

- Including the γ_c term plays a significant role in simulating the well-mixed boundary layer structure BUT the magnitude only minor influence

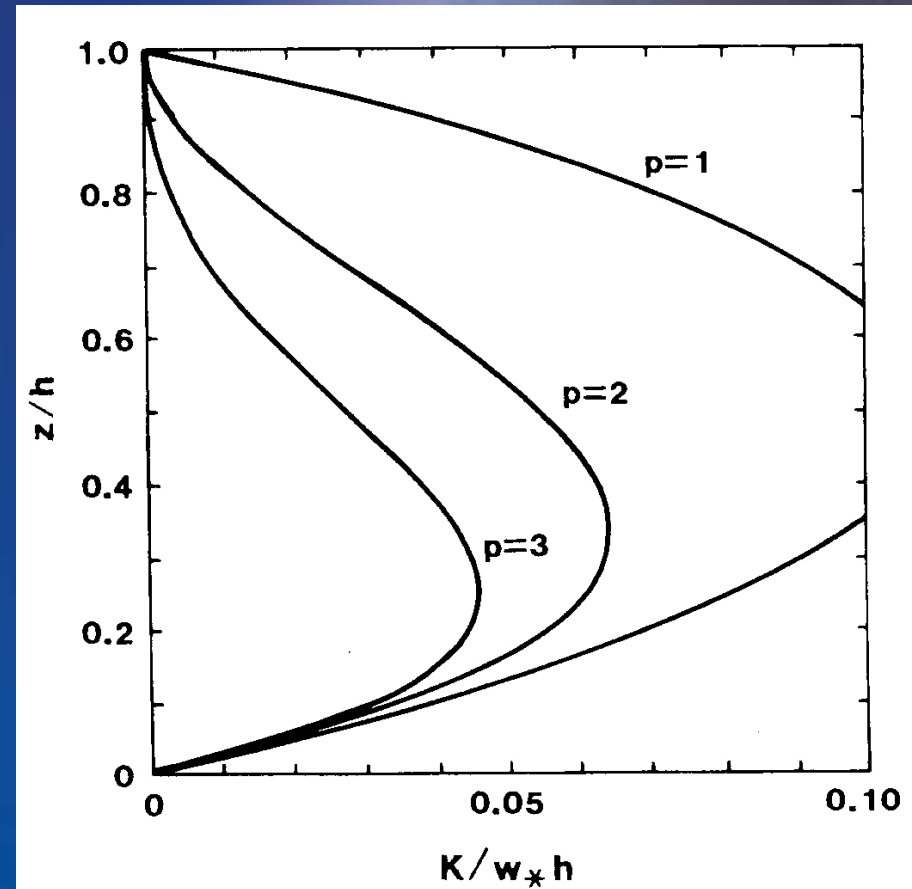
a) AUG 9&10 at 2145 UTC



Sensitivity Analysis

Examine impact of diffusivity profile shape (p term):

- Impact of p is similar to the γ_c mixing because an increase from 2 to 3 results in a reduction of the boundary layer top mixing due to less entrainment flux



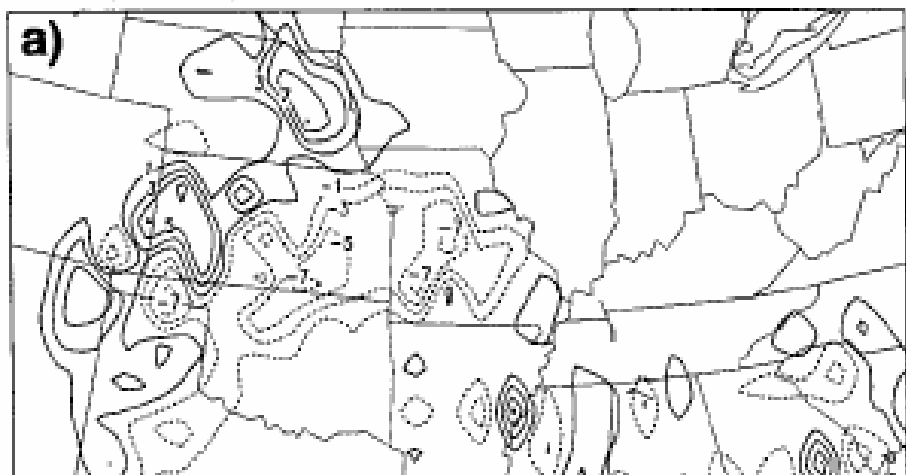
Troen and Mahrt 1986

Sensitivity Analysis

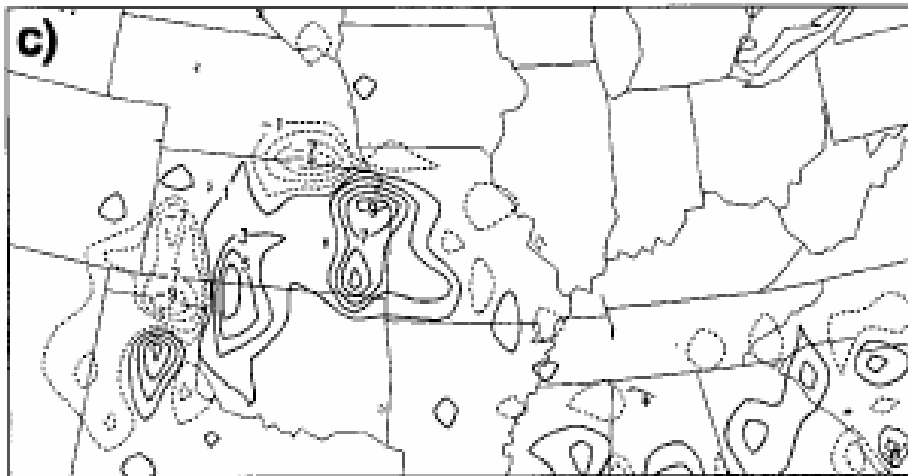
Sensitivity of boundary layer height on critical Richardson number:

- Impact of R_{ibcr} in precipitation forecast was found to be significant on heavy rain case for 15-17 May 1995
- Less effective mixing with lower PBL height (due to lower R_{ibcr}) most likely leads to similar precipitation as local scheme
- However, nonlocal experiment with $R_{ibcr} = .75$ shows more organized precipitation and more effective mixing and gives favorable boundary layer structure
- As surface heating decreases, R_{ibcr} becomes more important in determining PBL depth which results in different BL top entrainment

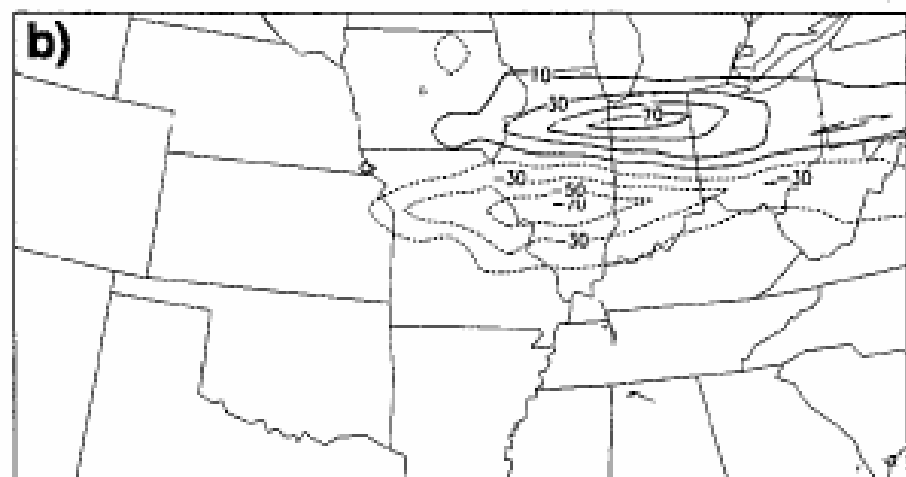
Precip Diff(mm) at 12Z 16, ND(.25)-ND(.50)



Precip Diff(mm) at 12Z 16, ND(.75)-ND(.50)



Precip Diff(mm) at 12Z 17, ND(.25)-ND(.50)



Precip Diff(mm) at 12Z 17, ND(.75)-ND(.50)

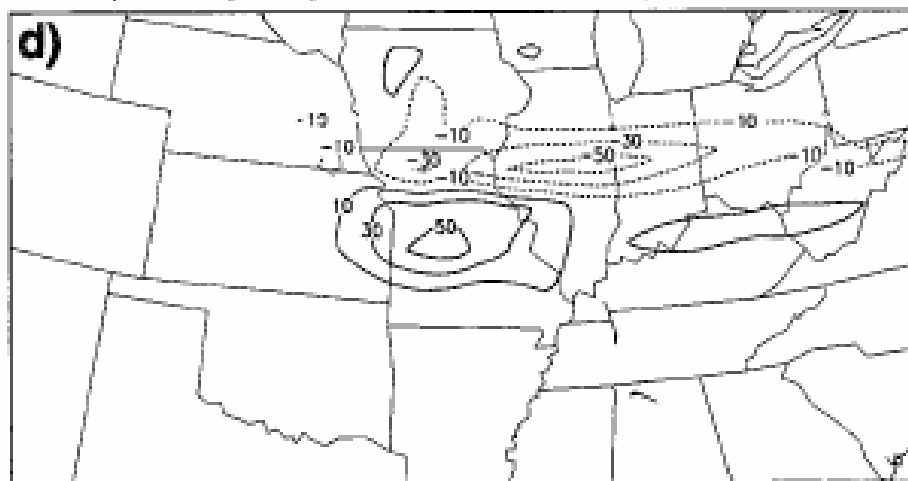


FIG. 12. The differences in precipitation between the control nonlocal scheme experiment with $Rib_{cr} = 0.50$ and the results using $Rib_{cr} = 0.25$ at the (a) 24-h and (b) 48-h forecasts, and the corresponding differences (c) and (d) from the results using $Rib_{cr} = 0.75$.

Hong and Pan, 1996

Summary MRF PBL parameterization

- Local diffusion scheme uses eddy diffusivity determined independently at each point in the vertical based on local vertical gradients wind and virtual potential temperature
- Nonlocal scheme determines eddy-diffusivity profile based on diagnosed BL height and turbulent velocity scale and it incorporates the nonlocal transport effects of heat and moisture (γ_c)
- MRF PBL equations derived from “Golden days” observations taken either from Kansas 1968 (Businger et al., 1971) or Minnesota 1973 (Kaimal et al., 1975).

Summary MRF PBL parameterization

- Impact on BL structure shows R_{bcr} and thermal excess (b) are negligible compared to the countergradient term and p factor for profiles of potential temperature and mixing ratio BUT not the same for precipitation field
- In the heavy precipitation case, Hong and Pan (1996) found that the rainfall is significantly affected by modifying the R_{bcr} , p profile, and countergradient term.
- However, should be able to tune the scheme by changing R_{bcr} only to get reasonable precipitation forecasts

References

- Troen and Mahrt, 1986: A Simple Model of the Atmospheric Boundary Layer; Sensitivity to Surface Evaporation. *Bound. Lay. Met.*, Vol. 37, pg. 129-148.
- Hong and Pan, 1996: Nonlocal Boundary Layer Vertical Diffusion in a Medium Range-Forecast Model. *Mon. Wea. Rev.*, Vol. 124, pg. 2322-2339.
- Brost and Wyngaard, 1978: A Model Study of the Stably Stratified Planetary Boundary Layer. *J. Atmo. Sci.*, Vol. 35, pg. 1427-1440.
- Businger et.al, 1971: Flux-Profile Relationships in the Atmospheric Surface Layer. *J. Atmo. Sci.*, Vol. 28, pg. 181-189.
- Holtslag and Boville, 1993: Local Versus Nonlocal Boundary Layer Diffusion in a Global Climate Model. *J. Atmo. Sci.*, Vol. 6, pg. 1825-1842.
- Wyngaard and Brost, 1984: Top-Down and Bottom-Up Diffusion of a Scalar in the Convective Boundary Layer. *J. Atmo. Sci.*, Vol. 41, pg. 102-112.
- Wyngaard, 1975: Modeling the Planetary Boundary Layer - Extension to the Stable Case. *Bound. Lay. Met.*, Vol. 9, pg. 441-460.
- WRF model Browser Code: <http://box.mmm.ucar.edu/wrf/WG2/wrfbrowser/>

Questions?

Melissa Goering
ATMO 595E
December 2, 2004